

# Spectroscopic binaries among Hipparcos M giants<sup>\*,\*\*</sup>

## I. Data, orbits, and intrinsic variations

B. Famaey<sup>\*\*\*,1</sup>, D. Pourbaix<sup>†,1</sup>, A. Frankowski<sup>‡,1</sup>, S. Van Eck<sup>†,1</sup>, M. Mayor<sup>2</sup>, S. Udry<sup>2</sup>, and A. Jorissen<sup>1</sup>

<sup>1</sup> Institut d'Astronomie et d'Astrophysique, Université libre de Bruxelles, Faculté des Sciences, CP. 226, Boulevard du Triomphe, B-1050 Bruxelles, Belgium

<sup>2</sup> Observatoire de Genève, Université de Genève, CH-1290 Sauverny, Switzerland

Received date; accepted date

### ABSTRACT

**Context.** This paper is a follow-up on the vast effort to collect radial velocity data for stars belonging to the Hipparcos survey.

**Aims.** We aim at extending the orbital data available for binaries with M giant primaries. The data presented in this paper will be used in the companion papers of this series to (i) derive the binary frequency among M giants and compare it to that of K giants (Paper II) and (ii) analyse the eccentricity – period diagram and the mass-function distribution (Paper III).

**Methods.** Keplerian solutions are fitted to radial-velocity data. However, for several stars, no satisfactory solution could be found, even though the radial-velocity standard deviation is greater than the instrumental error, because M giants suffer from intrinsic radial-velocity variations due to pulsations. We show that these intrinsic radial-velocity variations can be linked with both the average spectral-line width and the photometric variability.

**Results.** We present an extensive collection of spectroscopic orbits for M giants with 12 new orbits, plus 17 from the literature. On top of these, 1 preliminary orbit yielded an approximate value for the eccentricity and the orbital period. Moreover, to illustrate how the large radial-velocity jitter present in Mira and semi-regular variables may easily be confused with orbital variations, we also present examples of pseudo-orbital variations (in S UMa, X Cnc, and possibly in HD 115521, a former IAU radial-velocity standard). Because of this difficulty, M giants involving Mira variables were excluded from our monitored sample. We finally show that the majority of M giants detected as X-ray sources are actually binaries.

**Conclusions.** The data presented in this paper considerably increase the orbital data set for M giants, and will allow us to conduct a detailed analysis of the eccentricity – period diagram in a companion paper (Paper III).

**Key words.** binaries: spectroscopic - stars: late-type

## 1. Introduction

When a mass-losing M giant is present in a binary system, the interaction of the wind of the giant with the companion gives rise to photometric activity or spectroscopic symbiosis (like in symbiotic stars, in VV Cephei-like systems, or in low-mass X-ray binaries like V2116 Oph) that make the system very conspicuous even far away. However, if the M giant does not lose large amounts of mass, the binary nature of the star will not be as conspicuous. Combined with M giants often exhibiting pulsations that cause intrinsic velocity variations, thereby confusing the search for orbital variations, it explains why so few spectroscopic binaries involving M giants are known so far. Indeed, the Ninth Catalogue of Spectroscopic Binary Orbits ( $S_{B9}$ ; Pourbaix et al. 2004) contains 2746 entries (query

in March 2007), among which only 32 systems involve M giants, and yet 21 of these are either well-known symbiotic systems or VV-Cephei-like systems.

Carquillat and collaborators have devoted a series of papers to spectroscopic binaries of spectral types F to M, but only 2 binaries with primaries of spectral type MIII were studied (Carquillat & Ginestet 1996; Prieur et al. 2006). Previously, Stephenson (1967) provided a list of 7 systems with composite spectra involving an M star. But it is the paper by Hinkle et al. (2002) that, to the best of our knowledge, has so far provided the most extensive list of spectroscopic binaries involving non-symbiotic M giants.

With the present paper, we start a series devoted to a detailed study of the properties of spectroscopic binaries involving an MIII primary. The number of such binaries with known orbital elements has nearly doubled, as a result of our observing campaign of an extensive sample of M giants, drawn from the Hipparcos Catalogue, for which CORAVEL radial velocities have been obtained in a systematic way (Udry et al. 1997). The main driver behind this large database lies, of course, with the stellar kinematics in our Galaxy. And indeed the kinematical properties of the present sample of M giants have been fully analysed by Famaey et al. (2005) and Famaey et al. (2008). But this large data set may also be used to search for binaries.

The present paper presents the radial-velocity data (Sect. 2) and orbital elements (Sect. 4) of the newly-discovered spectro-

\* Based on observations carried out at the Swiss telescope installed at the *Observatoire de Haute Provence* (OHP, France), and at the 1.93-m OHP telescope

\*\* Tables 2, 3, and 6 are only available in electronic form at the CDS via anonymous ftp to cdsarc.u-strasbg.fr (130.79.128.5) or via <http://cdsweb.u-strasbg.fr/cgi-bin/qcat?J/A+A/>

\*\*\* Postdoctoral Researcher, F.N.R.S., Belgium

† Research Associate, F.N.R.S., Belgium

‡ Postdoctoral Researcher, F.N.R.S., Belgium. Currently at Department of Physics, Technion-Israel Institute of Technology, Haifa 32000, Israel

scopic binaries, for which a satisfactory orbit could be obtained. It also discusses the intrinsic variations sometimes mimicking orbital variations (Sect. 3). The list of new orbital elements is complemented with an exhaustive list of orbital elements for non-symbiotic M giants drawn from the literature (Table 8). In Paper II (Frankowski et al. 2009), we will use the observational information gathered in this paper to derive the frequency of spectroscopic binaries among M giants, and compare it with that of K giants. Paper III (Jorissen et al. 2009) will then present an in-depth analysis of the eccentricity–period diagram for M giants.

## 2. Radial-velocity data

The basic sample of M giants is drawn from the Hipparcos survey stars (identified by flag 'S' in field H68 of the Hipparcos catalogue; ESA 1997). These M giants were extracted from the Hipparcos survey stars on the basis of the spectral type provided in the Hipparcos catalogue and of the absolute magnitude  $M_{H_p} < 4$  computed from the Hipparcos parallax and  $H_p$  magnitude. Mira stars or supergiants of luminosity class I (when explicitly mentioned in the spectral classification) were not included in the sample (notably because of the confusion that their envelope pulsation may cause on the radial-velocity variations). This first sample (defined here as sample I) contains 771 M giants with declinations greater than  $-15^\circ$  and corresponds to the sample of northern M giants analysed in Famaey et al. (2005), to which 65 M giants with declinations between 0 and  $-15^\circ$  have been added. Two radial-velocity measurements, spanning at least one year, have been obtained with the CORAVEL spectrovelocimeter (Baranne et al. 1979) for all stars of sample I, as part of a monitoring programme targeting all Hipparcos survey stars later than about F (Udry et al. 1997). Note that 22 objects of the sample of Famaey et al. (2005) are not present in sample I because they had only one radial velocity measurement, making them unsuitable for binarity analysis. Famaey's sample was also screened for other irregularities, such as wrong Hipparcos spectral type or mistaken identity<sup>1</sup>. Extrinsic S stars were removed from the sample as well.

Subsamples of sample I have been subject to more intensive observing campaigns. Every third star from this sample has received a denser coverage, with (mostly) 4 instead of 2 measurements (7 stars received only 3 measurements), to achieve a better binary detection rate: this subsample of sample I is defined as sample II. Figure 1 displays the histograms of  $N_{\text{meas}}$  (the number of measurements per star),  $\langle \epsilon \rangle$  (average uncertainty of one measurement), and  $\Delta t$  (time spanned by the measurements of a given star) for the 254 stars of sample II.

Furthermore, 35 stars from sample II, suspected of being binaries (i.e., with a radial-velocity standard deviation  $\sigma(V_r) > 1 \text{ km s}^{-1}$  at the end of the observing campaign of sample II) have been monitored with the ELODIE spectrograph (Baranne et al. 1996) at the Haute-Provence Observatory to derive their orbital elements. They make up sample III. At the end of the ELODIE monitoring, a late measurement was obtained for 157 stars from sample II with  $\sigma(V_r) < 1 \text{ km s}^{-1}$  (this selection being mainly based on right ascension), in order to detect binaries with very

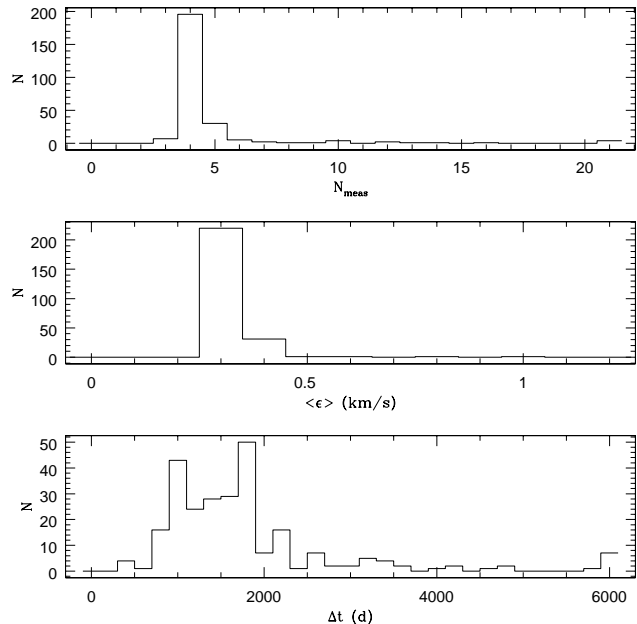


**Fig. 1.** Histograms of the number of measurements per star ( $N_{\text{meas}}$ ), the average uncertainty of one measurement ( $\langle \epsilon \rangle$ ), and the time spanned by the measurements of a given star ( $\Delta t$ ), for sample II (see Tables 1 and 2).

**Table 2.** The first five lines of the list of stars from sample II. The full table is only available electronically at the CDS.

HD	$N_{\text{tot}}$	$N_{\text{ELO}}$	$V_r$	$\sigma(V_r)$	$\epsilon(V_r)$	$Sb^a$	flag <sup>b</sup>
			( $\text{km s}^{-1}$ )	( $\text{km s}^{-1}$ )	( $\text{km s}^{-1}$ )	( $\text{km s}^{-1}$ )	
1013	5	1	-46.67	0.18	0.26	2.80	-
1255	5	1	14.57	0.32	0.27	3.95	-
2313	5	1	24.15	0.18	0.28	3.15	-
2411	6	2	4.67	1.06	0.25	4.58	ORB
2637	5	1	11.25	0.19	0.25	1.33	-

<sup>a</sup> The average sigma of a Gaussian fitted to the cross-correlation profile, corrected for the instrumental width ( $7 \text{ km s}^{-1}$  for CORAVEL at the Haute-Provence Observatory);

<sup>b</sup> The flag in this column is the same as in Table 4.

long orbital periods. These constitute sample IV. A summary of the properties of these four samples is presented in Table 1.

The CORAVEL data were put on the ELODIE radial-velocity system to ensure homogeneity (Udry et al. 1999b). The uncertainty  $\langle \epsilon \rangle$  of one radial-velocity measurement is approximately  $0.3 \text{ km s}^{-1}$  for CORAVEL measurements, but is better for ELODIE measurements. With the ELODIE single-fibre mode used during the present observing campaigns, it may be as good as  $50 \text{ m s}^{-1}$  (Baranne et al. 1996). It was not measured in a systematic way; however, to fix the ideas, an accuracy of  $0.2 \text{ km s}^{-1}$  has been associated with the ELODIE measurements in the data files.

The data for sample I (average velocity, radial-velocity standard deviation, and binarity flag) may be found in Table A.1<sup>2</sup>

<sup>1</sup> The only mistake found in Famaey et al. (2005) was the star HIP 26247 = RR Cam = BD +72°275, which was wrongly assigned radial velocity measurements from the binary star J275 in the Hyades cluster. The former star should therefore be discarded from the CORAVEL sample.

<sup>2</sup> As a result of the confusion between HIP 26247 and a binary star (see footnote 1), the star HIP 26247 is erroneously flagged as a binary in that table.

**Table 1.** The four observing campaigns defining the four (sub)samples of Hipparcos M giants.

Sample	I	II	III	IV
Selection	2 measurements in Famaey et al. (2005)	~1/3 of I	all $\sigma(V_r) > 1 \text{ km s}^{-1}$ from II	$\sigma(V_r) < 1 \text{ km s}^{-1}$ from II $0^h \leq \alpha \leq 16.5^h$
$N_{\text{star}}$	771	254	35	138
$N_{\text{meas}}$ per star	2	$\geq 4^a$	$\geq 5$	$N(\text{II})+1$
Telescope	Swiss 1-m (OHP)	Swiss 1-m (OHP)	1.93-m (OHP)	1.93-m (OHP)
Spectrograph	CORAVEL	CORAVEL	ELODIE	ELODIE
Time span	1991–1999	1993–1995	2000–2004	2001–2004

<sup>a</sup> Seven stars have  $N_{\text{meas}} = 3$ .

**Table 3.** The individual radial-velocity measurements for the 35 stars of sample III. The full table is available electronically from the CDS, Strasbourg.

HD	JD–2 400 000	$V_r$	$\epsilon(V_r)$	Inst <sup>a</sup>
2411	48876.599	4.97	0.32	COR
2411	49223.556	6.05	0.33	COR
2411	49668.360	6.42	0.31	COR
2411	50717.506	4.74	0.32	COR
2411	52304.297	3.56	0.20	ELO
2411	53047.246	4.39	0.20	ELO
4301	48441.832	6.36	0.28	COR
4301	49309.361	7.08	0.29	COR
4301	49581.863	6.96	0.27	COR
4301	49602.549	6.58	0.29	COR
4301	53048.254	4.50	0.20	ELO
...				

<sup>a</sup> A flag identifying the spectrograph: COR = CORAVEL; ELO = ELODIE; CAM = Cambridge spectrovelocimeter

(columns 24–26) of Famaey et al. (2005). A similar table, merging CORAVEL and ELODIE data, is given in Table 2 for sample II, which also provides the binarity diagnostics (according to the rules that will be specified in Sect. 3.1). Individual radial-velocity measurements for the 35 stars of sample III are given in Table 3. Roger Griffin has kindly provided us with supplementary measurements for HD 182190 and HD 220088 that allowed us to compute an orbit for these two stars. These measurements were performed with his Cambridge spectrovelocimeter and are listed in Table 3, with the label ‘CAM’. To put them on the ELODIE system, an offset of  $-0.8 \text{ km s}^{-1}$  has been applied.

### 3. Binaries, intrinsic radial-velocity jitter, and pseudo-orbits caused by pulsation

#### 3.1. Binarity diagnostic

The search for spectroscopic binaries (SBs) among M giants is made difficult by the bulk mass motion existing in the atmospheres of these stars (all M giants being variable to some extent; e.g. Eyer & Grenon 1997; Jorissen et al. 1997; Soszyński et al. 2004), since such motion triggers some intrinsic radial-velocity jitter<sup>3</sup> (e.g., Udry et al. 1998; Hinkle et al. 2002). This intrinsic jitter amounts to nearly  $1.5 \text{ km s}^{-1}$  in the coolest (non-Mira) M giants<sup>4</sup> (Fig. 2), so the detection of SBs cannot rely

<sup>3</sup> A term introduced by Gunn & Griffin (1979) in this context.

<sup>4</sup> Mayor et al. (1984) have shown that stars located at the tip of the giant branch in the globular cluster 47 Tuc have a jitter of  $\sim 1.25 \text{ km s}^{-1}$ , while the jitter reduces to  $0.27 \text{ km s}^{-1}$  for 1 mag-fainter stars. This trend

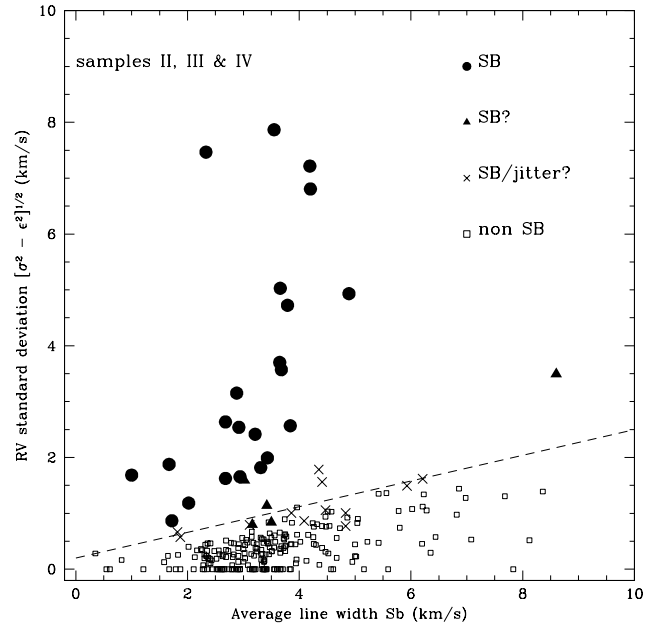


**Fig. 2.** The radial-velocity standard deviation  $\sigma_0(V_r)$  as a function of the average intrinsic line width  $Sb$ , for samples II, III, and IV (see Table 1). For non-binary stars (open squares), the maximum radial-velocity jitter increases with  $Sb$ . The dashed line represents a rough division between binary and non-binary stars. How this line has been defined will be discussed in Paper II. Symbols are as indicated in the figure.

solely on a  $\chi^2$  test comparing the radial-velocity standard deviation  $\sigma(V_r)$  to the average instrumental error  $\langle \epsilon \rangle$ . In the following, we denote by  $\sigma_0(V_r)$  the radial-velocity standard deviation corrected for the average instrumental error  $\langle \epsilon \rangle$ , i.e.  $\sigma_0(V_r) = (\sigma^2(V_r) - \langle \epsilon \rangle^2)^{1/2}$ .

In a first step, to flag a star as a binary in samples II, III, and IV, we therefore rely solely on the visual examination of the radial-velocity variations, and whether or not it is possible to obtain a meaningful orbital solution. The binarity diagnostic is then complemented by two criteria, described in detail in Sects. 3.1.1 and 3.1.2: (i) the location of the star in a diagram  $\sigma_0(V_r) - Sb$  (Fig. 2), where  $Sb$  denotes the intrinsic width of spectral lines (Sect. 3.1.1), and (ii) its location in a diagram  $\sigma_0(V_r) - \sigma(Hp)$  (Fig. 3), where  $\sigma(Hp)$  is the standard deviation of the Hipparcos magnitude (Sect. 3.1.2). The final binarity diagnostic for all stars

goes further down the red-giant branch, as shown with much higher accuracy levels by Setiawan et al. (2004) and da Silva et al. (2006).

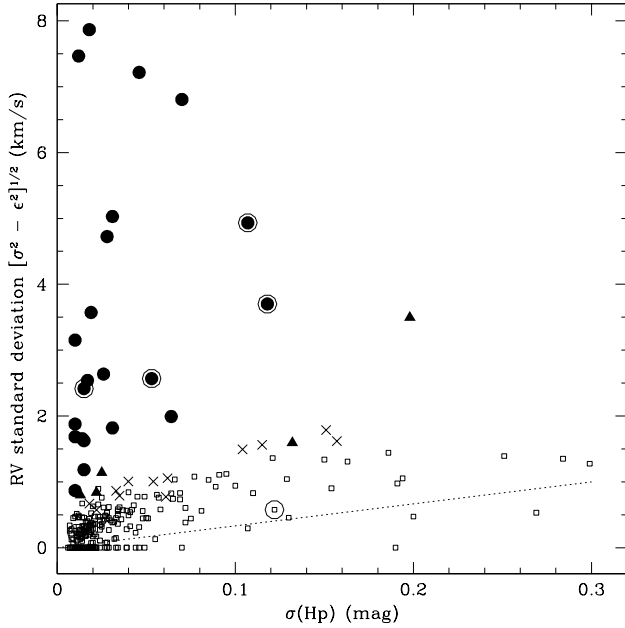


**Fig. 3.** The radial-velocity standard deviation (corrected for the instrumental error) as a function of the standard deviation on the Hipparcos  $H_p$  magnitude. Symbols are the same as in Fig. 2, except that large circles identify stars detected as X-ray sources by the ROSAT All-Sky Survey, following Hünsch et al. (1998). The dotted line represents the trend between radial-velocity and photometric variability reported by Hinkle et al. (1997). This is *not* a dividing line like the one plotted in Fig. 2.

from sample III (and for stars from sample IV, which are SB or suspected SB) is listed in Table 4 according to the following categories:

- a “ORB” : a satisfactory orbit could be computed (see Fig. 4);
- b “ORB:” : the orbit is preliminary, because the number of data points or the time coverage are not large enough, or two different solutions are possible (see Fig. 4);
- c “SB” : the star is a spectroscopic binary, but there are not enough data points to even compute a preliminary orbit (see Fig. 5);
- d “SB?” : the star is suspected to be a binary (see Fig. 6), even though it falls close to the dividing line in the  $\sigma_0(Vr)\text{--}Sb$  diagram (see Sect. 3.1.1 and Fig. 2).
- e “SB / jitter?” : it is not clear whether the radial velocity variations are of intrinsic or extrinsic nature (see Fig. 7): the star falls close to the dividing line in the  $\sigma_0(Vr)\text{--}Sb$  diagram (Fig. 2).

The radial-velocity variations (of intrinsic nature) of non-SB stars of sample III are plotted in Fig. 8.

### 3.1.1. Intrinsic width of spectral lines

We note that the parameter  $Sb$ , measuring the intrinsic width of spectral lines, provides useful guidance in distinguishing radial-velocity jitter from orbital motion. This parameter is defined as  $Sb = (s^2 - s_0^2)^{1/2}$ , where  $s$  is the standard deviation of a Gaussian fitted to the CORAVEL cross-correlation dip (see Baranne et al. 1979) and  $s_0$  the instrumental width ( $7 \text{ km s}^{-1}$  for CORAVEL at the Haute-Provence Observatory; for details

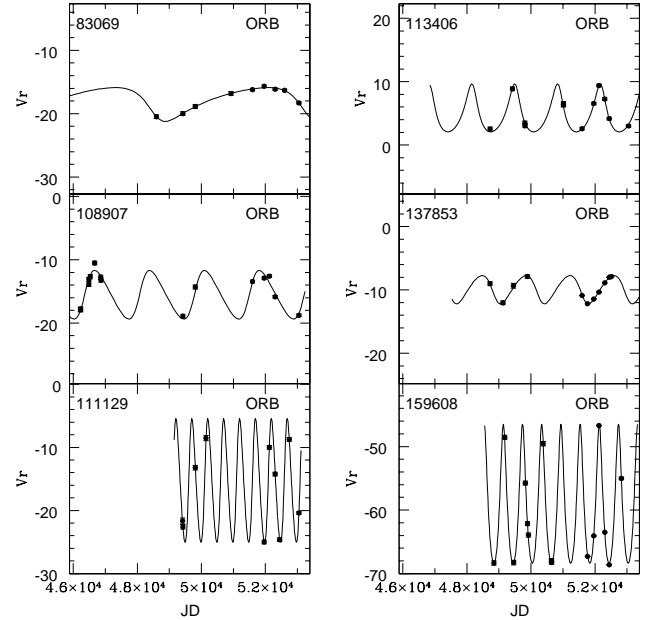


**Fig. 4.** Radial-velocity data points for the spectroscopic binaries, along with their orbital solution. The solution marked as ‘ORB:’ is not very well constrained and hence preliminary. All panels span a  $Vr$  range of  $30 \text{ km s}^{-1}$ . Error bars on the individual measurements (of the order of  $0.2 \text{ km s}^{-1}$ ) are too small to be seen.

see Jorissen & Mayor 1988; Van Eck & Jorissen 2000, also Paper II). Indeed, Fig. 2 reveals that stars for which no orbital solution could be found (open squares) have radial-velocity standard deviations that increase as  $Sb$  increases. In Paper II, we will show that  $Sb$  correlates closely with the stellar radius. We thus foresee that radial-velocity variations in stars falling well below the dashed line in Fig. 2 are most likely of intrinsic (rather than orbital) origin. Of course, binaries with an orbit seen almost face on, or with a long period, or insufficiently sampled, may also fall below the dashed line. Let us stress that the slope of this dividing line in Fig. 2 can be influenced by both the number of radial-velocity data points for a given object and the total number of objects in the sample (see Sect. 2.1 of Paper II).

Examples of radial-velocity variations for such stars from sample III, falling below the dividing line in Fig. 2, are plotted in Fig. 8, and it is clear that no orbital solution can be found for them. On the other hand, stars along the dashed line, whose velocity variations are plotted in Fig. 7, could either be SB or exhibit radial-velocity jitter. These 10 stars are listed in Table 4c.

On the other hand, among stars from samples III and IV, for which 5 or more measurements have been made, 22 certain spectroscopic binaries have been found, as listed in Table 4a. Of those, only 3 (HD 89758, HD 108907, and HD 132813) were previously known to be spectroscopic binaries, and a new satisfactory orbit could be computed for 12 of them (with the help of supplementary data points from the Cambridge spectrovelocimeter for HD 182190 and HD 220088; see Table 3). The orbital elements are presented in Sect. 4. The radial-velocity data points of the binary stars are displayed in Fig. 4 for those binaries with an orbit available (labelled in Table 4 as ORB or, for preliminary solutions, ORB:), and in Fig. 5 for the SBs without orbits. On top of the firm binaries, 5 stars were identified

**Table 4.** Binarity and photometric-variability diagnostics for stars from sample III (as well as binaries or suspected binaries from sample IV).

HD	$N$	$\Delta t$ (d)	Sp	$\sigma_0(Vr)$ (km s <sup>-1</sup> )	$\langle \epsilon \rangle$ (km s <sup>-1</sup> )	$Sb$ (km s <sup>-1</sup> )	Flag	Rem.	GCVS <sup>a</sup>	Var.	$\sigma(Hp)$ (mag)	$P_{\text{phot}}$ (d)
83069	9	4450	M2III	1.63	0.22	2.68	ORB		NSV 04545		0.015	
89758	7	6632	M0III	3.57	0.25	3.68	ORB	<sup>b</sup>	NSV 04829	SR	0.019	
108907	15	6821	M4III	2.57	0.25	3.84	ORB		CQ Dra	CV	0.053	
111129	10	3633	M2III	6.81	0.23	4.20	ORB		BY CVn *	Irr	0.070	
113406	12	4324	M1III	2.54	0.23	2.94	ORB		*		0.017	
132813	5	3639	M4.5III	4.93	0.27	4.89	ORB	<sup>b</sup>	RR UMi	SR	0.107	43.3
137853	11	3794	M1III	1.66	0.22	2.94	ORB		*		0.014	
159608	16	3981	M2III	7.87	0.25	3.55	ORB		*		0.018	
165374	37	7349	M2III	5.03	0.33	3.61	ORB		V980 Her *	Irr	0.031	
182190	24	4197	M1III	3.15	0.22	2.88	ORB		*		0.010	
187372	16	5787	M1III	2.42	0.26	3.21	ORB		*		0.015	
199871	10	3964	M0III	7.47	0.24	2.33	ORB				0.012	
203525	10	4741	M0III	1.68	0.23	0.88	ORB :		*		0.010	
212009	9	5008	M0III	4.72	0.23	3.66	ORB		KT Aqr *		0.028	
212047	12	3984	M4III	7.22	0.22	4.19	ORB		PT Aqr	SR	0.046	
220088	15	4743	M0III	1.88	0.22	1.67	ORB		*		0.010	
4301	5	4607	M0III	1.18	0.25	2.02	SB		*		0.015	
16058	5	4443	M3III	3.70	0.26	3.65	SB		NSV 866	Lb:	0.118	
104216	5	3626	M2III	1.99	0.27	3.43	SB		FR Cam	L	0.064	
134627	5	3922	M0	1.82	0.28	3.31	SB		FF Boo *		0.031	
142804	5	4964	M1III	2.64	0.27	2.68	SB		NSV 7351	Irr	0.026	
219215	7	4741	M2III	0.87	0.24	1.72	SB	<sup>c</sup>	*		0.010	

<sup>a</sup> An asterisk in this column means that the variability of the star has been discovered by Hipparcos.

<sup>b</sup> HD 89758, HD 132813: an orbit is also available in the literature, as listed in Table 8.

<sup>c</sup> HD 219215: Preliminary orbital period: 2500 d

whose radial-velocity variations are very likely orbital (listed in Table 4b and displayed in Fig. 6).

### 3.1.2. Photometric variability

Although Mira stars have been excluded from our sample, some semi-regular variables are nevertheless present. Both classes of variables often exhibit pseudo-orbital variations caused by shock waves associated with the envelope pulsation (Udry et al. 1998; Hatzes & Cochran 1998; Wood 2000; Hinkle et al. 2002; Setiawan et al. 2004; Derekas et al. 2006; Soszyński 2007; Hekker et al. 2008). For semi-regular variables, Hinkle et al. (2002) obtain semi-amplitudes  $K$  between 1.6 and 3.1 km s<sup>-1</sup>, whereas for Miras the semi-amplitudes may reach 20 km s<sup>-1</sup> in the most extreme cases (Alvarez et al. 2001). In terms of standard deviations, these values become 1.1, 1.7, and 14 km s<sup>-1</sup>, respectively (remember that for sinusoidal variations,  $\sigma = K/\sqrt{2}$ ). Semi-regular and Mira variables may thus be expected to exhibit  $\sigma_0(Vr)$  values anywhere in the range of 1 to about 14 km s<sup>-1</sup>.

Moreover, the radial-velocity curves of these stars may often be fitted by a Keplerian orbit with a period of a few hundred days (Udry et al. 1998; Hinkle et al. 2002; Wood et al. 2004; Lebzelter et al. 2005). However, it happens that this Keplerian solution fits the data for 4 to 10 cycles, and then becomes invalid. Two illuminating examples of this kind of behaviour are discussed in the Appendix for stars that do not belong to the samples considered in this paper (the Mira S star S UMa and the

semiregular carbon star X Cnc). If the time span of the radial-velocity monitoring is not long enough (i.e., shorter than the 4 to 10 cycles mentioned above), the inadequacy of the Keplerian solution may not be noticed, thus leading to the erroneous suspicion of binarity.

It is therefore very important to check that the Keplerian solutions proposed in Sect. 4 hereafter are valid, by eliminating the possibility that they have an intrinsic origin, as often observed for Mira and semi-regular variables. For this purpose, we collected from the literature the photometric properties of all the stars listed in Table 4 (including those flagged as having ‘radial-velocity jitter’, among which we should expect to find a large fraction of photometric variables). We searched the Hipparcos Variability Annex, which has the advantage of being an unbiased information source containing all our stars. The results are plotted in Fig. 3 [ $\sigma(Hp)-\sigma_0(Vr)$  diagram], and listed in Table 4. As we can see, all stars flagged as spectroscopic binaries (Fig. 3), have much larger radial-velocity standard deviations than expected from the relation between radial velocity and photometric variability for single stars (as reported by Hinkle et al. 1997). We also see that this relation exhibits some scatter (Fig. 3), and that stars flagged as ‘SB/jitter?’ define a rough dividing curve between intrinsic and extrinsic radial velocity variations in the  $\sigma(Hp)-\sigma_0(Vr)$  diagram.

In the column ‘Var’ of Table 4, we see that almost all stars later than M3 are semi-regular (SR) variables, as expected. It is very clear that the fraction of SR variables with  $\sigma(Hp) > 0.05$  mag increases among stars with (or suspected of having) radial-velocity jitter. A specific case (HD 114961, marked as a

**Table 4.** (Continued).**b. Suspected binaries** (marked as black triangles in Figs. 2 and 3)

HD	$N$	$\Delta t$ (d)	Sp	$\sigma_0(Vr)$ (km s <sup>-1</sup> )	$Sb$ (km s <sup>-1</sup> )	Flag	Rem. <sup>a</sup>	GCVS	Var.	$\sigma(Hp)$ (mag)	$P_{\text{phot}}$ (d)
65275	9	4442	M0	0.84	3.50	SB?	III			0.022	
111946	9	5040	M1/2III	1.59	3.02	SB?	III	VW Crv*	Irr	0.132	45.6:
112142	5	4613	M3III	1.14	3.42	SB?	IV	$\psi$ Vir	Lb	0.025	
114961	5	4608	M7III	3.50	8.60	SB?	IV	SW Vir	SRb	0.198	150
189063	8	3642	M0III	0.80	3.16	SB?	III	<sup>d</sup> *		0.013	

**c. Binarity doubtful** (marked as crosses in Figs. 2 and 3)

5920	8	4157	M4III	0.77	4.83	SB/jitter?	III	AK Cet	Lb	0.061	
12292	5	4606	M5III	1.00	4.83	SB/jitter?	IV	AR Cet	SR:	0.054	
17491	6	4075	M5III	1.62	6.21	SB/jitter?	IV	Z Eri	SRb	0.157	80.0
24693	6	4762	M1III	0.79	3.11	ORB/jitter?	IV	<sup>b</sup> GO Eri		0.035	
66875	8	4034	M3III	1.06	4.47	ORB/jitter?	III	<sup>b</sup> BL Cnc	L	0.062	
75157	4	3626	M0	1.01	3.86	SB/jitter?	IV	FW Cnc*	Irr	0.040	
97876	9	4841	M4III	1.56	4.22	ORB/jitter?	III	UU Crt*	SR	0.115	
129902	5	4605	M1III	0.57	1.87	SB/jitter?	IV	<sup>c</sup> *		0.022	
149165	5	5087	M1III	0.67	1.82	SB/jitter?	IV	<sup>c</sup> *		0.018	
153698	12	4209	M4III	0.86	4.09	SB + jitter?	III	*		0.033	

**d. Non-SB (radial-velocity jitter)** (marked as open squares in Figs. 2 and 3)

2411	6	4171	M3III	1.03	4.58			TV Psc	SR	0.085	49.1
6262	9	3702	M3III	1.04	4.51			V360 And *	SR	0.066	
69229	7	4819	M1III	0.44	2.32					0.018	
80567	8	3627	M3	1.04	5.78			IN Hya	SRb	0.129	277.8
107397	9	3746	M3III	1.35	5.42			RY UMa	SRb	0.284	295.7
112264	6	3022	M5III	1.08	6.02			TU CVn	SRb	0.077	50.0
115322	9	3627	M6III	1.49	5.93			FH Vir	SR	0.104	70.0
124304	9	4361	M3III	0.90	5.05			EV Vir	SR	0.154	120.0
125357	8	4361	M2/3III	1.78	4.35			MZ Vir	Irr	0.151	
166253	10	3631	M0	1.11	3.96			V566 Her	SRb	0.091	137.0
186776	11	5981	M4III	0.94	4.47			V973 Cyg	SRb	0.100	40.0

<sup>a</sup> This column specifies whether the binarity suspicion resulted from campaign III or IV (see Table 1)

<sup>b</sup> HD 24693 and HD 66875: Orbital solutions with an eccentricity of about 0.5 and periods of  $845 \pm 7$  and  $668 \pm 4$  d, respectively, are possible, but their reality is questionable. The stars are irregular (Lb) variables (varying from  $Hp = 7.13$  to  $7.26$  and  $5.94$  to  $6.11$ , respectively, in the Hipparcos catalogue) falling right on the dividing line in Fig. 2.

<sup>c</sup> HD 129902 and HD 149165 are probably spectroscopic binaries, given their location in Fig. 2 just above the dashed line. Unfortunately, the radial-velocity data presented in Fig. 6 are too scarce to confirm that conclusion.

<sup>d</sup> HD 189063: Orbital period larger than 3600 d

suspected binary ‘SB?’ in Table 4) will be discussed in Sect. 3.3. Such stars are not very numerous among the ones flagged as SB. Therefore, one can be confident that all the stars flagged as SB in Table 4a are indeed binaries. Only two among those are semi-regular variables with large photometric amplitudes (i.e., HD 16058 = 15 Tri and HD 132813 = RR UMi), and there are good arguments in favour of their binary nature. HD 16058 is a newly flagged spectroscopic binary, but it is an X-ray source. As we show in Sect. 3.2, X-ray detection in M giants is a strong indication of binarity. The binary nature of HD 132813 has already been claimed by Dettmar & Giesekeing (1983) and Batten & Fletcher (1986), who obtained consistent orbital parameters (Table 8). Our recent radial-velocity measurements are consistent with these orbital parameters (see Fig. 9), thus clearly demonstrating the binary nature of HD 132813 from the stability of the Keplerian solution.

### 3.2. X-ray emission as binarity diagnostic

X-rays are normally not observed in single M giants lying to the right of the so-called dividing line, an almost vertical boundary in the HR diagram separating stars with hot coronae emitting X-rays (to the left) from stars with high mass loss (to the right), which are normally not X-ray emitters (Hünsch et al. 1998). Since X-rays may be generated by several physical processes in a binary system, their detection in an M giant is a strong argument in favour of its binary nature. First, X-rays may be produced at the shocks resulting from the collision of streams in the complex flow pattern associated with wind accretion in a detached binary system involving an AGB star (Theuns & Jorissen 1993; Theuns et al. 1996; Mastrodemos & Morris 1998; Jahanara et al. 2005). Second, X-rays are generated when the gravitational energy of the M giant

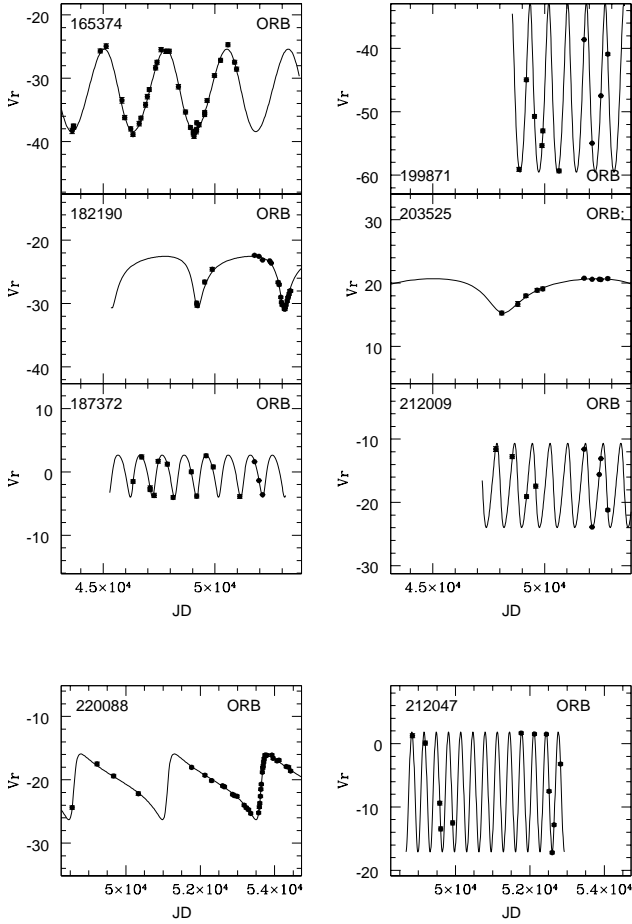


Fig. 4. Continued.

wind falling in the potential well of the companion star is converted into radiative energy when hitting the stellar surface. The accretion luminosity will either be radiated away in the form of hard X-rays if the infalling matter is optically thin; or if that matter is optically thick, half will be converted into thermal energy and half will be radiated away in the form of blackbody radiation (according to the virial theorem).

A search for X-ray sources among M giants is therefore an efficient way of finding binary systems. The ROSAT all-sky survey of X-ray sources detected only 11 out of 482 M giants of luminosity classes I to III from the *Bright Star Catalogue* (Hünsch et al. 1998). They are listed in Table 5, along with a comment regarding the binary nature. These few detections justify using radial-velocity variations to detect binaries among M giants in our paper.

It may be seen from Table 5 that, in most cases, the M giants detected as X-ray sources are flagged as binaries (4 from the present work, 1 from the literature, and 1 symbiotic). In three cases (HD 62898, HD 132813, and HD 155035), the X-ray source is offset by more than  $1'$  from the optical position of the giant, which casts doubts on the M giant being the source of the X-rays (see Hünsch et al. 1998, for details). In two other cases, there is a visual G-type companion, where X-rays may arise from coronal emission. Thus only HD 130144 and HD 150450 have no satisfactory explanation for the origin of the X-rays. In Fig. 3, it is HD 130144 that appears amidst the non-binary M giants.

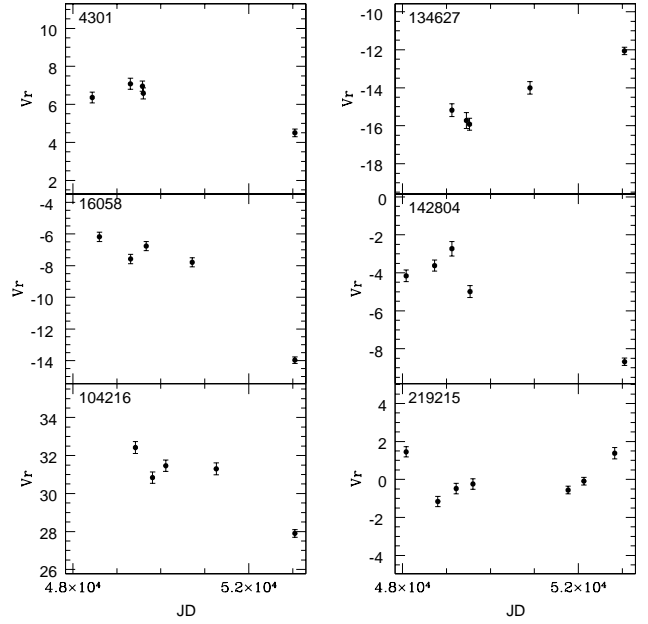


Fig. 5. Radial-velocity data points for the spectroscopic binaries with no orbit available yet.

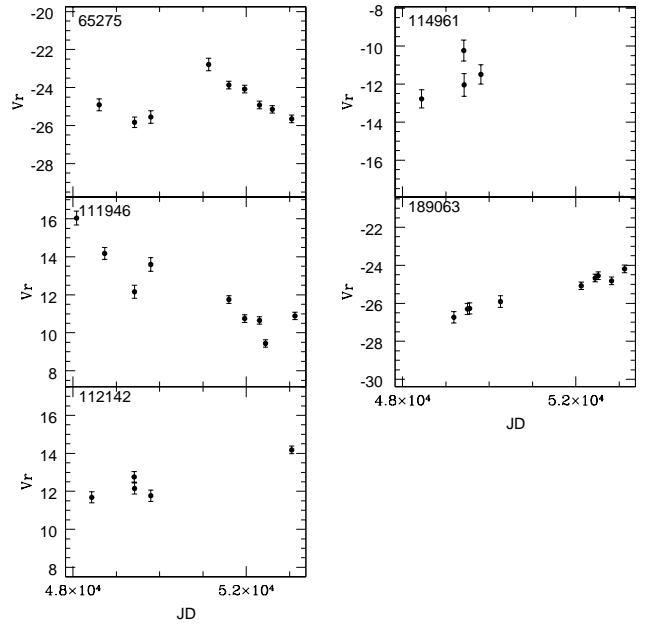
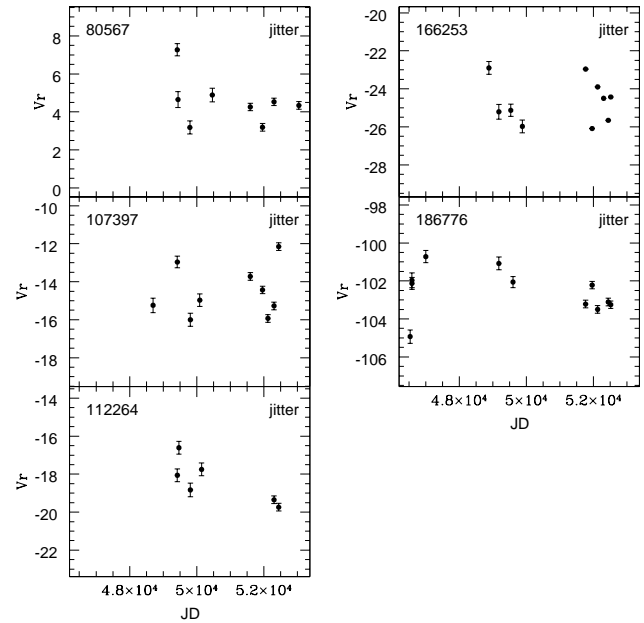
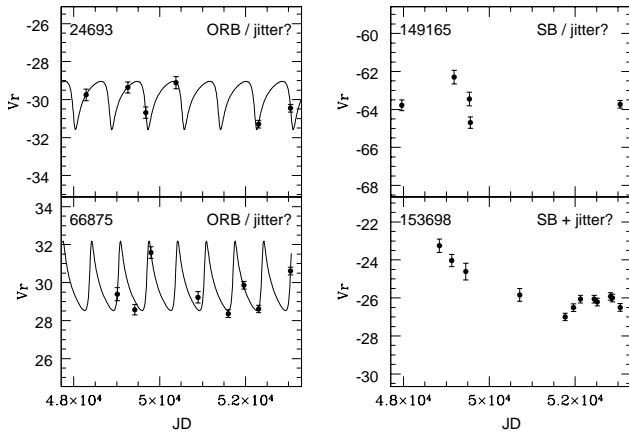
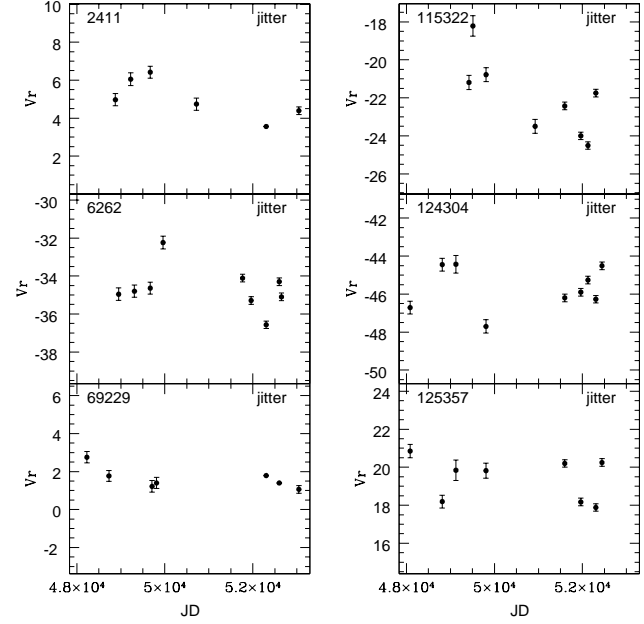
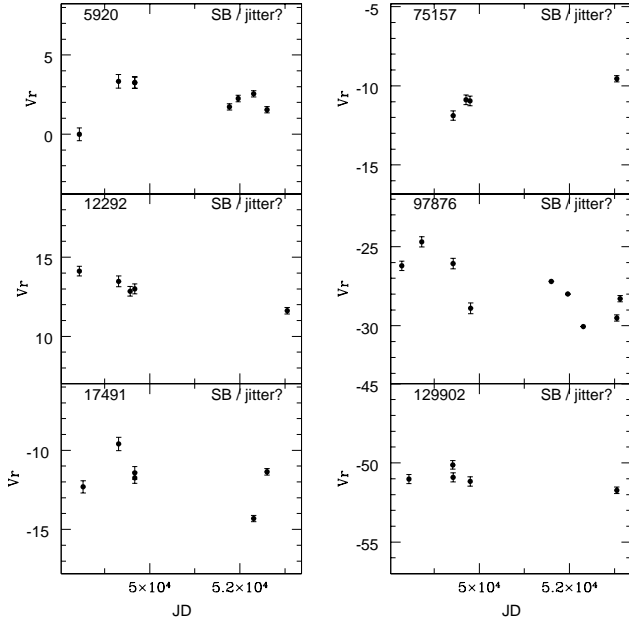


Fig. 6. Radial-velocity data points for the suspected spectroscopic binaries.

### 3.3. Special cases

#### 3.3.1. HD 114961

Since semi-regular and Mira variables may be expected to exhibit  $\sigma_0(Vr)$  values anywhere in the range from 1 to about  $14 \text{ km s}^{-1}$ , the value  $\sigma_0(Vr) = 3.1 \text{ km s}^{-1}$  observed for the semi-regular variable HD 114961 (SW Vir) in sample II is not incompatible with intrinsic variations (although we flagged it as a suspected binary; indeed, HD 114961 is the triangle in Fig. 2



**Fig. 7.** Radial-velocity variations for stars falling close to the dividing line between jitter and orbital motion in Fig. 2, for which the nature of the radial-velocity variations is unclear. The vertical scale spans  $10 \text{ km s}^{-1}$  in all cases. They are denoted by crosses in Fig. 2.

**Table 5.** Properties of the 11 M giants detected as X-ray sources by the ROSAT all-sky survey (following Hünsch et al. 1998), where for three stars, the X-ray source is offset by more than  $1'$  from the M giant optical position.

HR	HD	Name	Sp. Typ.	Binary?
750	16058	15 Tri	M3 III	SB
2216	42995	$\eta$ Gem	M3 III	ORB + visual GV comp.
3013	62898	$\pi$ Gem	M1 III	X-ray offset
4765	108907	4 Dra	M4 III	ORB
5512	130144	-	M5 IIIab	$V_r$ constant?
5589	132813	RR UMi	M4.5 III	ORB - X-ray offset
6200	150450	42 Her	M2.5 IIIab	
6374	155035	-	M1-2 III	X-ray offset
6406	156014	$\alpha^1$ Her	M5 Ib-II	visual GV companion
7547	187372	-	M1 III	ORB
8992	222800	R Aqr	M7 IIIpe	SB (symbiotic)

**Fig. 8.** Examples of radial-velocity variations for stars (referred to by their HD number, as listed in each panel) falling close to the dividing line between jitter and orbital motion in Fig. 2, with a radial-velocity jitter most likely of intrinsic nature. They are denoted by open squares in Figs. 2 and 3.

with the largest  $\sigma_0(V_r)$  for  $Sb = 8.5 \text{ km s}^{-1}$ ). Let us note, however, that the radial-velocity data available for this star are unfortunately too scarce to infer any periodicity, so no firm conclusion can be reached at this point regarding the intrinsic or orbital origin of the large radial-velocity scatter exhibited by SW Vir.



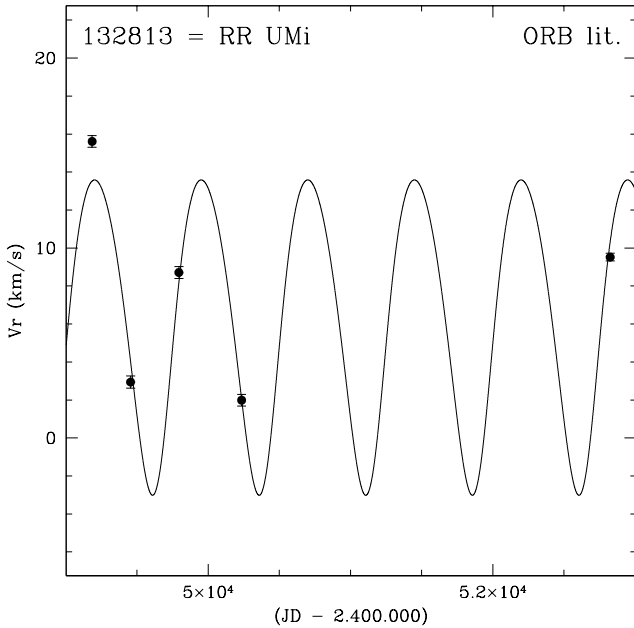


**Fig. 9.** Orbit from Batten & Fletcher (1986) for HD 132813. Overplotted are our new data points, consistent with this orbit from the literature, obtained about two decades ago.

### 3.3.2. HD 115521

HD 115521 is an interesting case, similar to those discussed in the appendix. It belongs to sample I (and therefore does not appear in Table 4 since it has only been measured twice in our observing campaign), but being a radial-velocity standard star till the 1990s (Udry et al. 1999a), it was measured very frequently and turned out in the first place to be variable with a small amplitude ( $K \sim 1.5 \text{ km s}^{-1}$ ) and a period around 500 d (Duquennoy & Mayor 1991). The 127 measurements are listed in Table 6, only available electronically at the CDS, Strasbourg. Later on, variations on a much longer time scale became apparent, exceeding the measurements' time span of 6358 d. The orbital period therefore cannot be determined with good accuracy. Moreover, owing to this insufficient sampling of the orbital cycle, the value adopted for the orbital period strongly influences the value derived for the eccentricity. Table 7 lists the (pseudo-)orbital elements used to draw the radial-velocity curve of Fig. 10. The high uncertainties on the elements of the long-period orbit should serve as a reminder that these elements are very uncertain. Only lower bounds to the orbital period and the eccentricity are therefore listed in Table 8.

The properties of the short-period variations would imply a rather low mass for the companion: assuming a mass of  $1.3 M_{\odot}$  for the giant, the minimum mass for the companion is  $0.054 M_{\odot}$ , corresponding to a brown dwarf. It is not entirely clear whether the short-period variations are indeed due to an orbital motion, for several reasons. First, as for S UMa and X Cnc discussed in the Appendix, the data deviate from the Keplerian solution after a dozen cycles, and this is very clearly seen in Fig. 10, where the first data points do not fall on the solution defined by later measurements. Second, with  $\log g = 0.70$  and  $K = 1.2 \text{ km s}^{-1}$  (Table 7), the short-period variations of HD 115521 fall on the  $\log g - K$  ( $K$  being the semi-amplitude of the radial-velocity variations) relationship as defined by Hekker et al. (2008) for

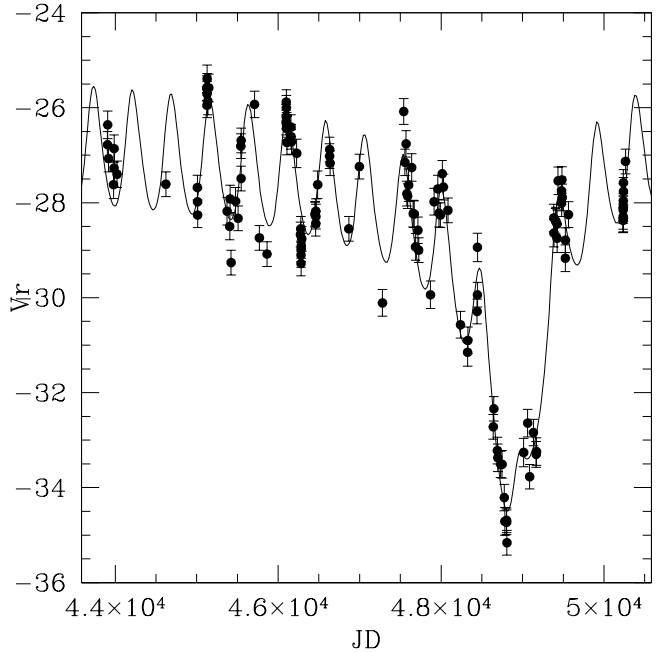


**Fig. 10.** The radial-velocity measurements of the former radial-velocity standard HD 115521. Short-term variations with a period of 475 d are superimposed on variations with a much longer time scale. The solid curve is obtained by adopting  $P = 29208 \text{ d}$  and  $e = 0.87$  for the long-period orbit.

K giants<sup>5</sup>. The existence of this relation between the amplitude of the radial-velocity variations and an intrinsic property of stars like the surface gravity hints at an *intrinsic* origin of such radial-velocity variations. The relation  $\log g - K$  found by Hekker et al. (2008) among K giants (initially suggested by Hatzes & Cochran 1998) continues in the domain of M giants, as we discuss in Paper II, where it is shown that the radial-velocity standard deviation correlates with the CORAVEL parameter  $Sb$  (measuring the spectral line width), which is in turn a good measure of the stellar radius (see Figs. 1 and 3 of Paper II).

However, if the shorter-period radial-velocity variations are intrinsic, then one expects photometric variations with a period of 475 d; unfortunately, we could not find any mention of them, in either the Catalogue of Suspected Variable Stars, where HD 115521 is entry NSV 6173, or in the Hipparcos Photometry Annex, or in the ASAS Catalogue of Variable Stars (Pojmański 2002).

## 4. Orbital elements of newly-discovered binaries

The complete set of orbital elements for the 12 newly discovered binaries are listed in Table 8. Figure 11 presents the phase diagrams for those firm orbital solutions. The second part of Table 8 provides a preliminary period and eccentricity for the binary with not enough data points to derive meaningful or-

<sup>5</sup> The gravity estimate is obtained as follows. From  $V = 4.80$  and the 2MASS value  $K = 0.47$ , one derives  $T_{\text{eff}} = 3680 \text{ K}$  and  $BC_K = 2.74$ , from the  $V - K$  calibrations of Bessell & Wood (1984) and Bessell et al. (1998). The maximum-likelihood distance of Famaey et al. (2005) ( $168 \pm 20 \text{ pc}$ ) then yields  $M_{\text{bol}} = -2.9$ , and a radius of  $84 R_{\odot}$  from the Stefan-Boltzmann relationship between luminosity,  $T_{\text{eff}}$  and radius. Adopting a mass of  $1.3 M_{\odot}$  then yields a gravity of  $\log g = 0.70$ .

**Table 6.** The 127 radial-velocity measurements for HD 115521. The table, only available at the CDS, Strasbourg, lists the Julian Date, the radial velocity, and the corresponding error.

**Table 7.** Orbital elements for the system HD 115521. It is not certain, however, that the short-period variations (A+a) are due to an orbital motion (see text). The long period orbit is not well-constrained.

	A+a	Aa+b
$V_\gamma$	$-26.93 \pm 2.1$	0
$P$ (d)	$475.1 \pm 1.4$	29000 :
$T_0$	$2\,449\,411 \pm 29$	$2\,419\,767 \pm 86282$
$e$	$0.148 \pm 0.062$	$0.87 \pm 0.24$
$\omega$ ( $^\circ$ )	$-27.1 \pm 22.9$	$191.8 \pm 3.5$
$K$ (km s $^{-1}$ )	$1.25 \pm 0.07$	$4.2 \pm 0.5$
$f(M)$ ( $M_\odot$ )	$9.3 \cdot 10^{-5}$	0.027
$a_1 \sin i$ (AU)	0.053	5.57
$\sigma(O - C) = 0.50 \text{ km s}^{-1}$		

Orbital solutions. For the sake of completeness, the last part of Table 8 collects periods, eccentricities, and mass functions for (non-symbiotic) M giants available in the literature, or kindly communicated by R. Griffin. This combined data set will be used in Paper III to discuss general properties (like the eccentricity–period diagram) of systems involving M giant primaries. It must be stressed that Table 8 includes orbits neither for symbiotics nor for VV-Cephei-like systems (VV Cep, AZ Cas, etc.). A list of orbital elements for the former may be found in Belczyński et al. (2000) and Mikołajewska (2003). Mikołajewska (2007) and Fekel et al. (2007) provide references for the most recent symbiotic orbits.

For HD 108907 (4 Dra = CQ Dra), Table 8 lists three orbital solutions. The first entry is obtained with our own CORAVEL and ELODIE data alone. The second entry is a solution computed by Reimers et al. (1988), based on their 57 recent data points plus 14 much older ones. The third orbit has been computed by merging our 15 data points with the 57 Cambridge/CORAVEL/Victoria data points from Reimers et al. (1988), and this combined solution is presented in Fig. 12. This system is of special interest, since Reimers (1985) and Reimers et al. (1988) argued that the companion of the red giant is a cataclysmic variable, because *International Ultraviolet Explorer* spectra revealed a steep rise shortward of 140 nm along with broad lines (full widths of 1000 km s $^{-1}$ ) of highly excited species like He II and C IV. That conclusion has been challenged, however, by more recent studies (Wheatley et al. 2003; Skopal 2005a,b) based on ROSAT X-ray observations. They conclude instead that the companion is a single WD accreting from the wind of its red giant companion, as in normal symbiotic systems. The residual radial-velocity jitter of 0.6 km s $^{-1}$  (listed as  $\sigma(O - C)$  in Table 8) appears normal for a star with  $Sb = 3.8 \text{ km s}^{-1}$ , as seen from Fig. 2.

*Acknowledgements.* The authors have the pleasure of thanking Roger Griffin for his generous donation of unpublished RV measurements for HD 182190 and HD 220088, which made it possible to compute their orbits. We are also indebted for his permission to quote in Table 5 several of his new orbits of M giants prior to their publication and for his helpful comments on the manuscript of this paper. We thank the referee, F. Fekel, whose comments greatly improved the paper, and in particular stimulated the addition of Fig. 3. This work has been partly funded by an *Action de recherche concertée (ARC)* from the *Direction générale de l'Enseignement non obligatoire et de la Recherche scientifique – Direction de la recherche scientifique – Communauté française de Belgique*.

## References

- Alvarez R., Jorissen A., Plez B., Gillet D., Fokin A., Dedecker M. 2001, A&A, 379, 305
- Baranne A., Mayor M., Poncet J. L. 1979, *Vistas in Astronomy*, 23, 279
- Baranne A., Queloz D., Mayor M., Adrianszyk G., Knispel G., Kohler D., Lacroix D., Meunier J.-P., Rimbaud G., Vin A. 1996, A&AS, 119, 373
- Batten A. H., Fletcher J. M. 1986, PASP, 98, 647
- Belczyński K., Mikołajewska J., Munari U., Ivison R. J., Friedjung M. 2000, A&AS, 146, 407
- Bessell M. S., Castelli F., Plez B. 1998, A&A, 333, 231
- Bessell M. S., Wood P. R. 1984, PASP, 96, 247
- Carquillat N., Ginestet J. M. 1996, A&AS, 117, 445
- da Silva L., Girardi L., Pasquini L., Setiawan J., von der Lühse O., De Medeiros J. R., Hatzes A., Döllinger M. P., Weiss A. 2006, A&A, 458, 609
- Derekas A., Kiss L. L., Bedding T. R., Kjeldsen H., Lah P., Szabó G. M. 2006, ApJ, 650, L55
- Dettmar R.-J., Giesekeing F. 1983, A&AS, 54, 541
- Duquennoy A., Mayor M. 1991, A&A, 248, 485
- ESA 1997, *The Hipparcos and Tycho Catalogues*, ESA
- Eyer L., Grenon M. 1997, in R. M. Bonnet, E. Høg, P. L. Bernacca, L. Emiliani, A. Blaauw, C. Turon, J. Kovalevsky, L. Lindegren, H. Hassan, M. Bouffard, B. Strim, D. Heger, M. A. C. Perryman, L. Woltjer (eds.), *Hipparcos - Venice '97*, Vol. 402 of *ESA Special Publication*, p. 467
- Famaey B., Jorissen A., Luri X., Mayor M., Udry S., Dejonghe H., Turon C. 2005, A&A, 430, 165
- Famaey B., Siebert A., Jorissen A. 2008, A&A, 483, 453
- Fekel F. C., Hinkle K. H., Joyce R. R., Wood P. R., Lebzelter T. 2007, AJ, 133, 17
- Frankowski A., Famaey B., Van Eck S., Jorissen A. 2009, A&A, this volume (Paper II)
- Frankowski A., Jancart S., Jorissen A. 2007, A&A, 464, 377
- Griffin R. F. 1979, *The Observatory*, 99, 198
- Griffin R. F. 1983, *The Observatory*, 103, 56
- Griffin R. F. 1990, *The Observatory*, 110, 85
- Griffin R. F. 2008, *The Observatory*, submitted
- Gunn J. E., Griffin R. F. 1979, AJ, 84, 752
- Hatzes A. P., Cochran W. D. 1998, in R. A. Donahue, J. A. Bookbinder (eds.), *Cool Stars, Stellar Systems, and the Sun*, Vol. 154 of *Astronomical Society of the Pacific Conference Series*, 311
- Hekker S., Snellen I. A. G., Aerts C., Quirrenbach A., Reffert S., Mitchell D. S. 2008, A&A, in press (astro-ph/0801.0741)
- Hinkle K., Lebzelter T., Joyce R., Fekel F. 2002, ApJ, 123, 1002
- Hinkle K. H., Lebzelter T., Scharlach W. W. G. 1997, AJ, 114, 2686
- Houk N. 1963, AJ, 68, 253
- Hünsch M., Schmitt J. H. M. M., Schröder K., Zickgraf F. 1998, A&A, 330, 225
- Jackson E. S., Shane W. W., Lynds B. T. 1957, ApJ, 125, 712
- Jahanara B., Mitsumoto M., Oka K., Matsuda T., Hachisu I., Boffin H. M. J. 2005, A&A, 441, 589
- Jorissen A., Frankowski A., Famaey B., Van Eck S. 2009, A&A, this volume (Paper III)
- Jorissen A., Mayor M. 1988, A&A, 198, 187
- Jorissen A., Mowlavi N., Sterken C., Manfroid J. 1997, A&A, 324, 578
- Lebzelter T., Hinkle K. H., Wood P. R., Joyce R. R., Fekel F. C. 2005, A&A, 431, 623
- Lucke P. B., Mayor M. 1982, A&A, 105, 318
- Lucy L. B., Sweeney M. A. 1971, AJ, 76, 544
- Luyten W. J. 1936, ApJ, 84, 85
- Mastrodemos N., Morris M. 1998, ApJ, 497, 303
- Mayor M., Benz W., Imbert M., Martin N., Prevot L., Andersen J., Nordstrom B., Ardeberg A., Lindgren H., Maurice E. 1984, A&A, 134, 118
- McLaughlin D. B., van Dijke S. E. A. 1944, ApJ, 100, 63
- Mikołajewska J. 2003, in R. L. M. Corradi, J. Mikołajewska, T. J. Mahoney (eds.), *Symbiotic stars probing stellar evolution*, *Astron. Soc. Pacific Conf. Ser.* Vol. 303, San Francisco, 9
- Mikołajewska J. 2007, *Baltic Astron.*, 16, 1
- Pojmański G. 2002, *Acta Astronomica*, 52, 397
- Pourbaix D., Tokovinin A. A., Batten A. H., Fekel F. C., Hartkopf W. I., Levato H., Morrell N. I., Torres G., Udry S. 2004, A&A, 424, 727
- Prieur J.-L., Carquillat J.-M., Griffin R. F. 2006, *Astronomische Nachrichten*, 327, 686
- Reimers D. 1985, A&A, 142, L16
- Reimers D., Griffin R. F., Brown A. 1988, A&A, 193, 180
- Reimers D., Schroeder K.-P. 1983, A&A, 124, 241
- Samus N. N. 1997, *Informational Bulletin on Variable Stars*, 4501, 1
- Setiawan J., Pasquini L., da Silva L., Hatzes A. P., von der Lühse O., Girardi L., de Medeiros J. R., Guenther E. 2004, A&A, 421, 241

**Table 8.** An extensive list of orbital elements for (non-symbiotic) M giants.**New orbits**

HD	Sp.	$N$	$\sigma(O-C)$ (km s <sup>-1</sup> )	$\Delta t$ (d)	$P$ (d)	$e$	$f(M)$ ( $M_{\odot}$ )	$T_0$ (JD -2 400 000)	$\omega$ ( $^{\circ}$ )	$K_1$ (km s <sup>-1</sup> )	$V_0$ (km s <sup>-1</sup> )	$a_1 \sin i$ (10 <sup>6</sup> km)
83069	M2III	9	0.11	4450	4768 ± 175	0.36 ± 0.12	0.0076	53 344 ± 106	132 ± 15	2.7 ± 0.2	-17.9 ± 0.1	163.3
108907	M4III	15	0.60	6821	1714 ± 4	0.20 ± 0.03	0.0094	53 239 ± 40	278 ± 9	3.8 ± 0.2	-15.6 ± 0.1	88.6 (1)
		71	0.90	24830	1703 ± 3	0.30 ± 0.05	0.0076	42 868 ± 40	244 ± 9	3.7 ± 0.2	-14.3 ± 0.1	82.0 (2)
		72	1.02	9451	1703 ± 3	0.33 ± 0.02	0.0063	53 204 ± 19	267 ± 4	3.5 ± 0.1	-14.8 ± 0.1	77.1 (3)
111129	M2III	10	0.18	3633	496.7 ± 0.7	0.14 ± 0.01	0.047	50 630 ± 17	299 ± 12	9.8 ± 0.3	-15.9 ± 0.1	66.3
113406	M1III	12	0.25	4324	1338 ± 7	0.30 ± 0.03	0.0065	50 865 ± 18	18 ± 5	3.8 ± 0.3	4.8 ± 0.1	66.4
137853	M1III	11	0.12	3794	1373 ± 15	0.15 ± 0.06	0.0015	51 616 ± 62	119 ± 17	2.2 ± 0.1	-9.8 ± 0.1	41.7
159608	M2III	16	0.39	3981	599.3 ± 0.4	0.22 ± 0.01	0.0751	52 731 ± 5	357 ± 3	10.9 ± 0.2	-59.9 ± 0.1	87.8
165374	M2III	37	0.41	7349	2741 ± 13	0.05 ± 0.02	0.0782	51 058 ± 128	74 ± 17	6.5 ± 0.1	-32.0 ± 0.1	245.3
182190	M1III	40	0.30	5258	3856 ± 22	0.57 ± 0.01	0.0155	53 053 ± 11	164 ± 2	4.1 ± 0.1	-24.4 ± 0.1	179.0
187372	M1III	16	0.36	5787	986 ± 3	0.24 ± 0.03	0.0034	50 201 ± 22	204 ± 8	3.3 ± 0.2	0.1 ± 0.1	43.8
199871	M0III	10	0.31	3964	840.2 ± 0.7	0.16 ± 0.02	0.203	51 899 ± 7	17 ± 3	13.4 ± 0.1	-48.2 ± 0.1	153.1
212009	M0III	9	0.17	5008	791.8 ± 1.1	0.17 ± 0.04	0.0231	53 529 ± 15	70 ± 6	6.6 ± 0.2	-17.7 ± 0.2	71.3
212047	M4III	12	0.24	3984	328.2 ± 0.1	0.016 ± 0.012	0.0290	49 315 ± 47	176 ± 53	9.4 ± 0.1	-7.5 ± 0.1	42.8
220088	M0III	37	0.13	5874	2516.6 ± 1.5	0.639 ± 0.004	0.0169	53 622.5 ± 2.6	259.5 ± 1.1	5.21 ± 0.05	-20.48 ± 0.03	138.9

- Skopal A. 2005a, in J.-M. Hameury, J.-P. Lasota (eds.), *The Astrophysics of Cataclysmic Variables and Related Objects*, Astron. Soc. Pac. Conf. Ser. (Vol.330), San Francisco, 463
- Skopal A. 2005b, *A&A*, 440, 995
- Soszyński I. 2007, *ApJ*, 660, 1486
- Soszyński I., Udalski A., Kubiak M., Szymański M., Pietrzyński G., Żebruń K., Szewczyk O., Wyrzykowski L. 2004, *Acta Astronomica*, 54, 129
- Stellingwerf R. F. 1978, *ApJ*, 224, 953
- Stephenson C. B. 1967, *PASP*, 79, 363
- Theuns T., Boffin H. M. J., Jorissen A. 1996, *MNRAS*, 280, 1264
- Theuns T., Jorissen A. 1993, *MNRAS*, 265, 946
- Tokovinin A. A. 1997, *A&AS*, 124, 75
- Udry S., Jorissen A., Mayor M., Van Eck S. 1998, *A&AS*, 131, 25
- Udry S., Mayor M., Andersen J., Crifo F., Grenon M., Imbert M., Lindgren H., Maurice E., Nordström B., Prévot L., Traversa G., Turon C. 1997, in M. Perryman (ed.), *Hipparcos - Venice '97* (ESA SP-402), ESA, Noordwijk, p. 693
- Udry S., Mayor M., Maurice E., Andersen J., Imbert M., Lindgren H., Mermilliod J., Nordström B., Prévot L. 1999a, in J. B. Hearnshaw, C. D. Scarfe (eds.), *Precise Stellar Radial Velocities*, Astron. Soc. Pacific Conf. Ser., Vol.170, San Francisco, 383
- Udry S., Mayor M., Queloz D. 1999b, in J. B. Hearnshaw, C. D. Scarfe (eds.), *Precise Stellar Radial Velocities*, Astron. Soc. Pacific Conf. Ser., Vol.170, San Francisco, 367
- Van Eck S., Jorissen A. 2000, *A&A*, 360, 196
- van Leeuwen F., Feast M. W., Whitelock P. A., Yudin B. 1997, *MNRAS*, 287, 955
- Verhoelst T., van Aarle E., Acke B. 2007, *A&A*, 470, L21
- Welty A. D., Wade R. A. 1995, *AJ*, 109, 326
- Wheatley P. J., Mukai K., de Martino D. 2003, *MNRAS*, 346, 855
- Wood P. R. 2000, *PASA*, 17, 18
- Wood P. R., Olivier E. A., Kawaler S. D. 2004, *ApJ*, 604, 800

no satisfactory fit can be found to the radial-velocity data. This star provides a good illustration of the difficulties encountered while trying to find spectroscopic binaries among long-period variable stars.

Figure A.1 shows the radial-velocity curve of S UMa and a (pseudo-)orbital solution based on 17 measurements (from 1987.946 to 2002.464 or JD 2 447 141.743 to JD 2 452 444.403; Tables A.1 and A.2). This pseudo-orbit is slightly different from the one found by Udry et al. (1998). Although the radial-velocity data could be fitted with a period of 576 d for 10 cycles, the last two measurements (JD 2 452 824.356 and JD 2 453 048.562) deviate markedly from this solution. The radial-velocity variations cannot therefore be ascribed to orbital motion. In any case, a system with such a short orbital period cannot be detached. Using the period-radius relationship for Mira stars pulsating in the fundamental mode (van Leeuwen et al. 1997), a radius of 258  $R_{\odot}$  is inferred from the 222-d period, assuming a mass of 1.5  $M_{\odot}$ . Adopting a mass of 1  $M_{\odot}$  for the companion, for the Roche radius to be larger than the stellar radius requires an orbital period of at least 1130 d, which is inconsistent with the observed value of 576 d.

What then is the origin of this 576 d period? The Stellingwerf (phase-dispersion minimisation)  $\theta$  statistics (Stellingwerf 1978) are shown in Fig. A.2, constructed from all datapoints but the last two outliers. It shows that all the prominent peaks are combinations of the Mira frequency  $f_1 = 1/222$  d<sup>-1</sup> and of the yearly frequency  $f_2 = 1/365.25$  d<sup>-1</sup>, or harmonics of  $f_1$ . In particular the 576 d period may be identified with the frequency  $f_1 - f_2$ . This finding, along with the previous result for the minimum period allowed by the Roche radius, definitely denies the reality of the binary nature of HD 110813. Alvarez et al. (2001) have shown that S UMa exhibits an asymmetric cross-correlation dip, as usual among Mira variables. Asymmetric profiles observed in Mira variables are often associated with radial-velocity variations, which indeed mimic an orbital motion (see also Hinkle et al. 2002).

## A.2. HD 76221

The semiregular carbon star HD 76221 (X Cnc) behaves similarly to HD 110813 (Udry et al. 1998): a satisfactory (pseudo-)orbital solution with a period of 530 d (Table A.1) could be found with the first 13 data points, but is not confirmed by the last two data points (bottom panel of Fig. A.1). The phase-dispersion minimisation statistics (Fig. A.3, based on the first 13 data points) reveals several harmonics of the 195 d photometric period, but this time, the 530-d periodicity of the radial velocities does not seem to be one of these. This 530-d-signal may be yet another example of the long secondary periods (of unknown origin) found by Houk (1963) (see also Hinkle et al. 2002) among SR variables, since the ranges of periods, mass functions, and semi-amplitudes found by Hinkle et al. (2002) (and listed in Table A.1) all match the values for HD 76221. Only the eccentricity does not conform to the Hinkle et al. range (0.32 – 0.37, with one case at 0.08). Soszyński (2007) also notes that the long secondary periods sometimes undergo phase shifts; however, we do not find it very plausible that these photometric and spectroscopic phase shifts have the same physical origin. The phase shifts in the light-curve are attributed by Soszyński (2007) to dust clouds in the vicinity of a

## Appendix A: Pseudo-orbits among Mira and semiregular variables

This Appendix presents two cases of (suspected) pseudo-orbital variations exhibited by Mira and semi-regular variables. These stars do not belong to the samples studied earlier in this paper.

### A.1. HD 110813

HD 110813 (S UMa) is a Mira S star with a light cycle of 225.9 d (as listed in the General Catalogue of Variable Stars – GCVS; the analysis below shows that a period of 222 d seems more appropriate), and was considered a spectroscopic binary of period 593 ± 62 d by Udry et al. (1998). It deserves a follow-up discussion here, since recent datapoints no longer support this orbital solution; in fact,

**Table 8.** (Continued.)**Preliminary orbit**

HD	Sp.	$N$	$\sigma(O-C)$	$\Delta t$ (d)	$P$ (d)	$e$	Rem.
203525	M0III	10	0.12	4741	7290:	0.4:	

**Orbits from the literature**

HD	Sp.	$P$ (d)	$e$	$f(M)$ ( $M_{\odot}$ )	Ref.
9053	M0III	193.8	0.0	0.083	$\gamma$ Phe: Luyten (1936)
41511	M4III	$260.34 \pm 1.80$	$0.024 \pm 0.005$	$0.261 \pm 0.005$	(4)
42995	M3III	2983	0.53	0.13	$\eta$ Gem: McLaughlin & van Dijke (1944)
80655	gM	834	0.0	0.0074	Griffin (1983)
89758	M0III	$230.089 \pm 0.039$	$0.061 \pm 0.022$	0.01	$\mu$ UMa: Jackson et al. (1957); Lucy & Sweeney (1971)
108815	M	$4448 \pm 20$	$0.73 \pm 0.03$	$0.012 \pm 0.003$	Griffin, priv. comm.
111307	M0	$18000 \pm 3000$	0:	$0.10 \pm 0.04$	Griffin, priv. comm.
115521Aa+b	M2III	> 7000	> 0.5	..	Sect.3.3.2
115521A+a		$475.1 \pm 1.4$	$0.15 \pm 0.06$	$9.3 \cdot 10^{-5}$	(5), revised but orbital nature doubtful (Sect. 3.3.2)
117673	M0III	$1360.8 \pm 2.3$	$0.26 \pm 0.02$	0.0095	Griffin (2008)
126947	M3III	$2812.3 \pm 9.4$	$0.432 \pm 0.021$	0.045	Prieur et al. (2006)
132813	M4.5III	748.9	0.13	0.0043	RR UMi (SRb, $P = 43.3$ d): Dettmar & Giesekeing (1983); Batten & Fletcher (1986)
147395	M2III	335.5	0.24	0.154	Carquillat & Ginestet (1996)
187076	M2II+late B	$3704.2 \pm 3.2$	$0.45 \pm 0.01$	$0.135 \pm 0.005$	Griffin, priv.comm. $\delta$ Sge: A $\zeta$ Aur/VV Cep-like system (Reimers & Schroeder 1983)
190658	M2.5III	198.7	0.05	0.045	(6)
192867	M1III	5929	0.64	0.032	Griffin (1990)
220007	M3III	1520	0.51	0.013	Griffin (1979)

Remarks: (1) this work (2) Reimers et al. (1988) (3) combined solution (see text) (4) SS Lep: M4III + accreting A1 star (Welty & Wade 1995). Verhoelst et al. (2007) shows, from interferometric measurements of the M-giant radius, that the giant fills its Roche lobe (see also Paper III) (5) Possibly a triple system, formerly a radial-velocity standard star; Duquennoy & Mayor (1991) found a preliminary 509 d period for the inner pair, but the orbital nature of the short-period variations is questionable (Sect. 3.3.2) (6) HD 190658 = V1472 Aql = HIP 98954: semiregular or most likely eclipsing or ellipsoidal variable with  $P = 100.37$  d, almost exactly half the orbital period (Samus 1997). Orbital elements from Lucke & Mayor (1982). A (physical?) companion is present at 2.3'' (Tokovinin 1997; Frankowski et al. 2007)

companion, whereas the phase shifts in radial velocity preclude the orbital nature of the radial velocity variations.

**Table A.1.** Pseudo-orbital solutions for the Mira S star HD 110813 (S UMa) and the semi-regular carbon star HD 76221 (X Cnc), based on the complete data set but the last two points (see Table A.2).

	HD 110813	HD 76221	LSP <sup>a</sup>
$P_{\text{puls}}$ (d)	222	195	
' $P_{\text{orb}}$ ' (d)	$576 \pm 1.9$	$530 \pm 8.9$	300 – 1000
$e$	$0.29 \pm 0.09$	0	0.08, 0.32 – 0.37
$\omega$ ( $^{\circ}$ )	$178 \pm 17$	–	240 – 320
$T$ (JD – 2 400 000)	$52839 \pm 23$	$44541 \pm 75$	
$K$ (km s <sup>-1</sup> )	$8.5 \pm 0.6$	$1.6 \pm 0.2$	1.6 – 3.1
$V_0$ (km s <sup>-1</sup> )	$3.6 \pm 0.5$	$-5.9 \pm 0.1$	
$f(M)$ ( $M_{\odot}$ )	$3.2 \cdot 10^{-2}$	$(2.3 \pm 0.9) \cdot 10^{-4}$	$2 \cdot 10^{-4} - 1.3 \cdot 10^{-2}$
$a_1 \sin i$ (10 <sup>6</sup> km)	64.4	$11.8 \pm 1.5$	
$N$	17	13	
$\sigma(O - C)$ (km s <sup>-1</sup> )	1.82	0.44	

<sup>a</sup> The ranges found by Hinkle et al. (2002) for semi-regular variables with long secondary periods.

**Table A.2.** Radial velocities for HD 76221 and HD 110813.

JD – 2 400 000	$V_r$ (km s <sup>-1</sup> )	$\epsilon$ (km s <sup>-1</sup> )	$O - C$ (km s <sup>-1</sup> )	Instr.
<b>HD 76221</b>				
48245.634	-4.07	0.37	+0.20	COR
48328.471	-4.98	0.34	-0.05	COR
48348.421	-5.48	0.34	-0.21	COR
48652.522	-5.57	0.36	+0.33	COR
48657.563	-5.57	0.34	+0.23	COR
48695.451	-6.16	0.36	-1.07	COR
49063.382	-7.71	0.32	-0.21	COR
49084.380	-7.45	0.33	-0.07	COR
49365.587	-4.42	0.40	+0.19	COR
49455.376	-6.24	0.54	-0.06	COR
49755.526	-4.56	0.38	+0.52	COR
50041.685	-6.85	0.35	+0.25	COR
50071.650	-7.34	0.35	+0.06	COR
50359.680	-6.17	0.34	–	COR
50362.648	-6.34	0.33	–	COR
<b>HD 110813</b>				
47141.743	0.94	0.58	+3.38	COR
47972.573	9.02	0.65	-0.49	COR
47996.476	9.35	0.40	+0.14	COR
48334.584	1.66	0.58	-0.41	COR
48349.556	2.21	0.57	-1.22	COR
48719.460	0.73	0.46	-0.24	COR
48753.455	1.29	0.50	+4.35	COR
49091.467	9.12	0.46	-0.48	COR
49100.422	10.17	0.54	+0.56	COR
49422.565	-4.02	0.37	+1.13	COR
49454.561	-2.51	0.74	-1.09	COR
49753.604	9.42	0.98	+0.87	COR
49808.417	6.09	0.51	-0.12	COR
51597.5	-1.0	0.40	-2.22	ELO
51652.5	-7.7	0.40	-2.46	ELO
52304.611	-7.36	0.40	-2.39	ELO
52444.403	8.04	0.40	+0.68	ELO
52824.356	-3.02	0.40	–	ELO
53048.562	-1.65	0.40	–	ELO

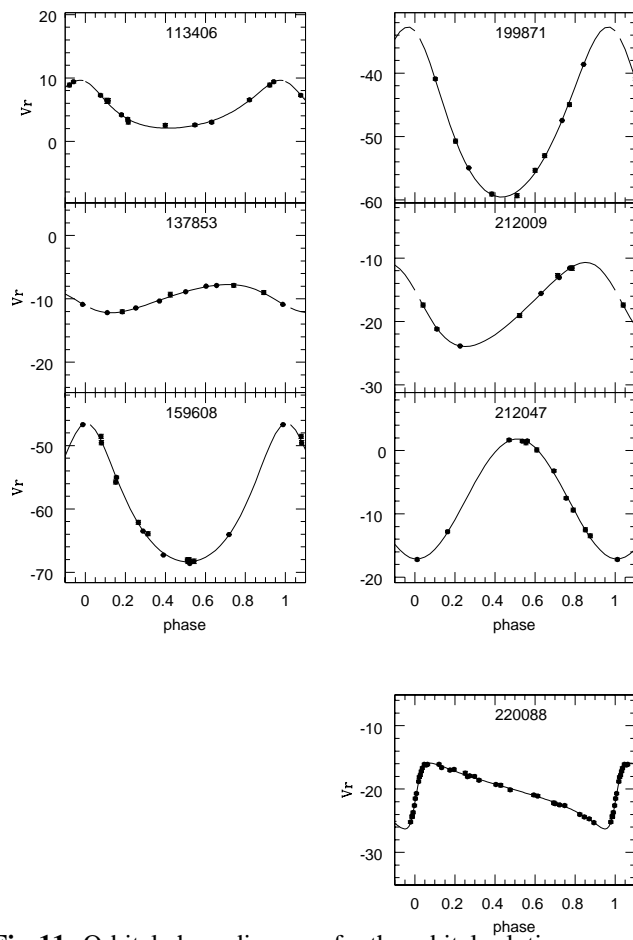
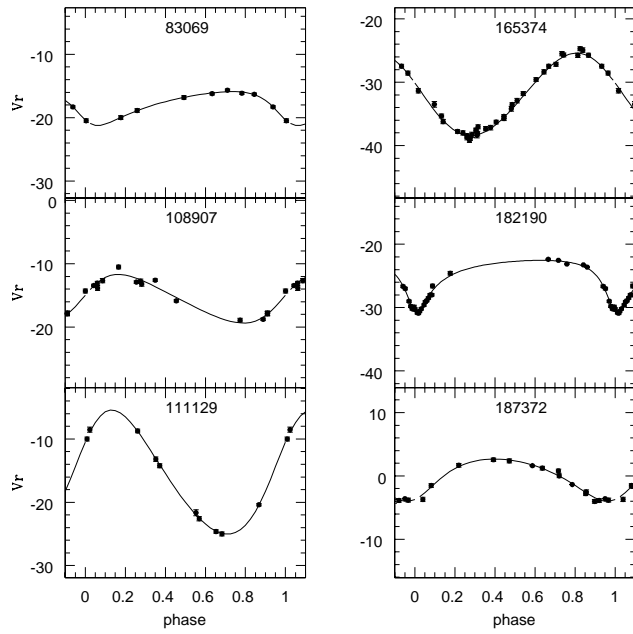


**Fig. 11.** Orbital phase diagrams for the orbital solutions, according to the solutions listed in Table 8.

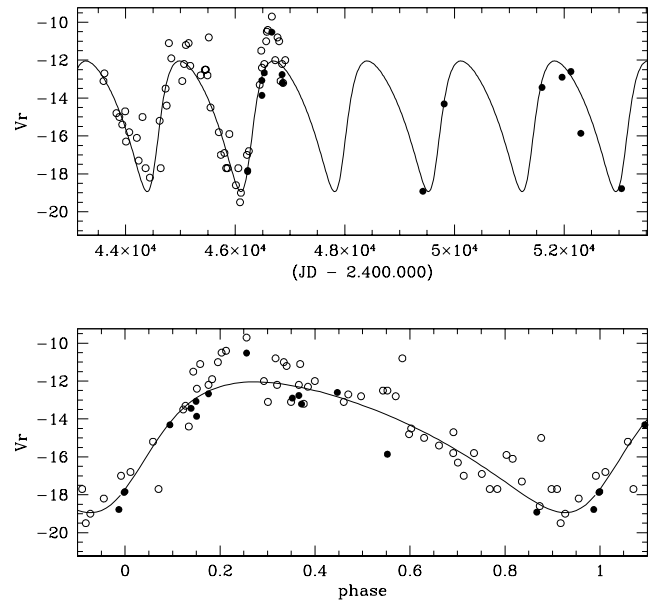


**Fig. 12.** Top panel: Radial-velocity curve for HD 108907 (4 Dra), an M giant with a hot compact companion, merging 57 data points from the Cambridge, Victoria, and CORAVEL spectrometers listed in Reimers et al. (1988) (open symbols) and the 15 data points from this paper (filled symbols). Bottom panel: Phase diagram for the orbital solution merging these two data sets.

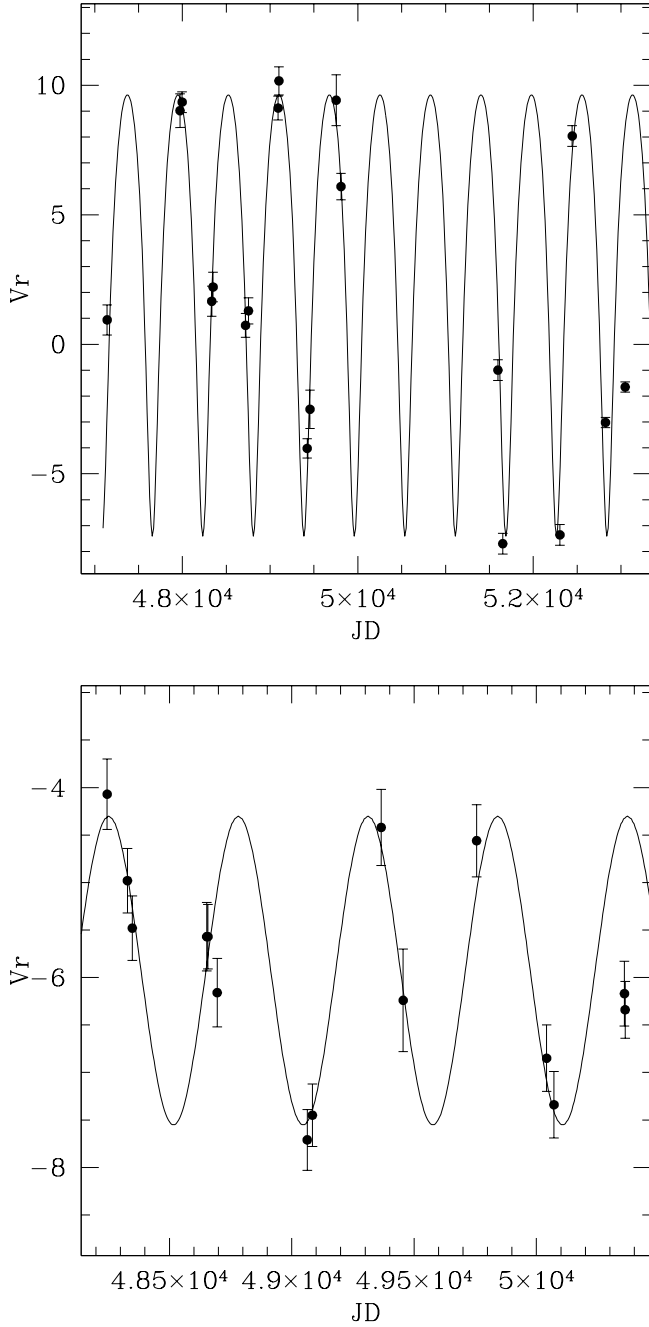


**Fig. A.1.** Top panel: Radial-velocity curve for HD 110813, a Mira S star with a pulsation period of 225.9 d (according to GCVS) and a pseudo-orbital period of 576 d. Bottom panel: Same for the carbon star HD 76221, a semi-regular variable with a pulsation period of about 195 d (according to GCVS), and a pseudo-orbital period of 530 d. For both stars, the last measurements become discrepant with the (pseudo-)orbital solution computed from earlier data points.

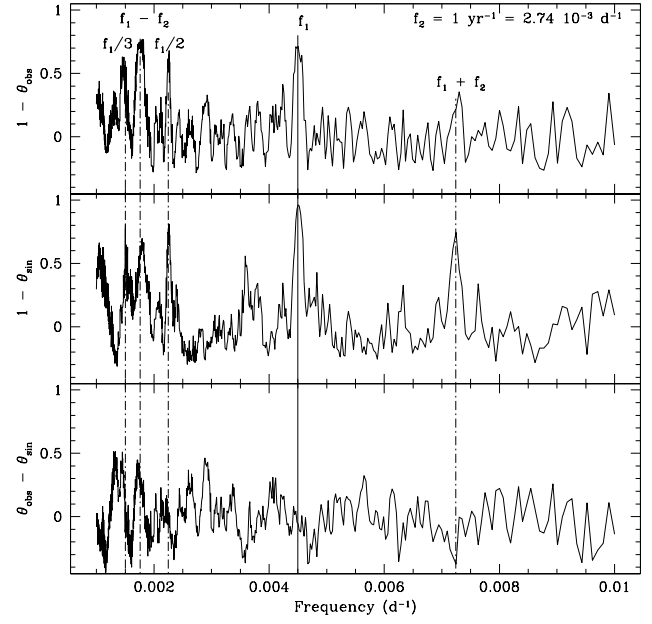


**Fig. A.2.** Top panel: Stellingwerf's  $1 - \theta$  statistics (with bins of length 0.2 phase cycle offset by 0.1 phase cycle from the previous one;  $N_b = 5$  and  $N_c = 2$  adopting Stellingwerf's notations), for all data points of HD 110813 (S UMa) but the last two (outliers). Middle panel: the  $1 - \theta$  statistics for a sinusoidal signal of period  $1/f_1 = 222$  d (corresponding to the Mira pulsation period) sampled as the data. Bottom panel: the difference between the former two, revealing peaks not accounted for by the aliases associated with the 222-d Mira period. In the top panel, several linear combinations of  $f_1$  (the Mira frequency) and  $f_2$  (the 1-yr frequency) are indicated. The pseudo-orbital period of 576 d is close to  $(f_1 - f_2)^{-1} = 555$  d.

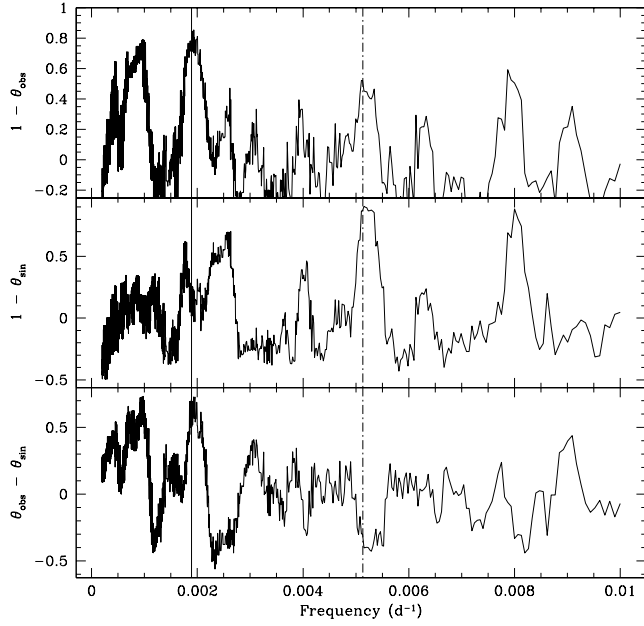


**Fig. A.3.** Top panel: Same as Fig. A.2 for the carbon star HD 76221, for all data points but the last two (outliers). The solid vertical line marks the frequency of the pseudo-orbital variation and the dot-dashed line the frequency of light variations. The harmonics  $1/3$ ,  $1/2$ ,  $3/4$ , and  $3/2$  of the pulsation frequency  $1/195 = 5.1 \cdot 10^{-3} \text{ d}^{-1}$  are clearly identifiable in the middle and top panels. Because there is a residual peak remaining in the lower panel at the pseudo-orbital frequency of  $1/530 = 1.9 \cdot 10^{-3} \text{ d}^{-1}$ , this frequency does not belong to this series of harmonics.